

ANGEWANDTE CHEMIE

A Journal of the
Gesellschaft
Deutscher Chemiker

INTERNATIONAL EDITION

2001
40/24

Pages 4519–4882



**Cover Picture
of the Year**
Cast your vote at
www.angewandte.com
and win a great book!

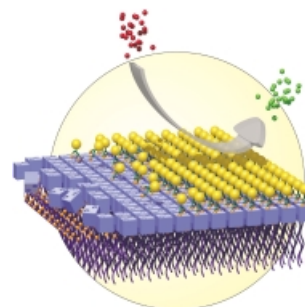


*The editorial staff and
the publishers thank all
readers, authors,
referees, and advertisers
for their interest and
support over the past
year and wish them all
a happy new year.*



COVER PICTURE

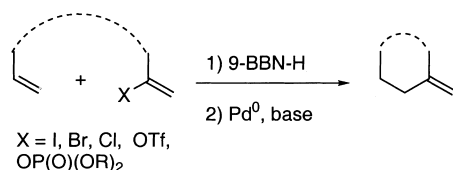
The cover picture shows the process of building functional amphiphilic protein–polymer hybrids in a modular fashion. Monolayers of biotinylated polystyrene (purple) bind the protein streptavidin (blue), resulting in the formation of giant amphiphiles. The remaining free binding sites are subsequently used to associate biotinylated biomacromolecules (yellow), such as the iron-storage protein ferritin. The use of covalent conjugates of streptavidin and horseradish peroxidase leads to the formation of reactive surfaces, which are capable of catalyzing organic reactions. Further details on these giant amphiphiles are reported by Nolte and co-workers on p. 4732 ff.



REVIEWS

Contents

An extremely attractive method for forming $C(sp^3)–C(sp^2)$ bonds in complex molecular settings is the *B*-alkyl Suzuki–Miyaura reaction (see scheme; 9-BBN-H = 9-borabicyclo[3.3.1]nonane; the dashed line indicates that intramolecular reactions are also possible). The regio-, chemo-, and stereoselective nature of this reaction has been used in a number of syntheses of natural and non-natural compounds. An intricate knowledge of the mechanism of this reaction provides the basis for future advancements in this field.



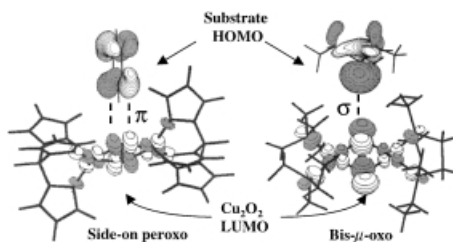
Angew. Chem. 2001, 113, 4676–4701

S. R. Chemler, D. Trauner,
S. J. Danishefsky* 4544–4568

The *B*-Alkyl Suzuki–Miyaura Cross-Coupling Reaction: Development, Mechanistic Study, and Applications in Natural Product Synthesis

Keywords: boranes • C–C coupling • cross-coupling • Suzuki–Miyaura coupling • synthetic methods

Copper enzymes are involved in dioxygen binding, activation, and reduction to water. The oxygen intermediates in these enzymes exhibit unique spectroscopic features, which reflect new geometric and electronic structures that play key roles in catalysis. Structure/function correlations are developed and reaction mechanisms are defined on a molecular level. The figure shows the calculated frontier orbitals of the μ - η^2 : η^2 -side-on bridged-peroxo Cu_2^{II} and the bis- μ -oxo- Cu_2^{II} intermediates, which activate π and σ electrophilic attack on substrates, respectively.



E. I. Solomon,* P. Chen, M. Metz,
S.-K. Lee, A. E. Palmer 4570–4590

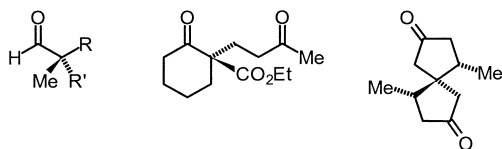
Oxygen Binding, Activation, and
Reduction to Water by Copper Proteins

Keywords: bioinorganic chemistry •
copper • electronic structure •
metalloenzymes • oxygen activation •
reaction mechanisms

Angew. Chem. **2001**, *113*, 4702–4724

MINIREVIEW

The synthesis of optically active natural products and pharmaceuticals with quaternary stereocenters is a particular challenge. The potential of new stoichiometric and catalytic asymmetric reactions can be proved by their suitability for the enantioselective generation of such fully substituted carbon centers, such as, for example, in the compounds shown.



Angew. Chem. **2001**, *113*, 4725–4732

J. Christoffers,* A. Mann . . . 4591–4597

Enantioselective Construction of
Quaternary Stereocenters

Keywords: asymmetric catalysis •
C–C coupling • chiral auxiliaries •
enantioselectivity • synthetic methods

VIPs

The following communications are “Very Important Papers” in the opinion of two referees. They will be published shortly (those marked with a diamond will be published in the next issue). Short summaries of these articles can be found on the *Angewandte Chemie* homepage at the address <http://www.angewandte.com>

Cesiumauride Ammonia (1/1), $\text{CsAu} \cdot \text{NH}_3$: A Crystalline Analogue of Alkali Metals Dissolved in Ammonia?

A.-V. Mudring, M. Jansen,*
J. Daniels, S. Krämer,
M. Mehring, J. P. Prates Ramalho,
A. H. Romero, M. Parrinello ◆

Enantiopure Double-Helical Alkynyl Cyclophanes

D.-L. An, T. Nakano, A. Orita,
J. Otera* ◆

Supramolecular Cluster Catalysis: Benzene Hydrogenation Catalyzed by a Cationic Triruthenium Cluster under Biphasic Conditions

G. Stüss-Fink,* M. Faure,
T. R. Ward ◆

The First Disulfur and Diselenium Complexes of Platinum: Syntheses and Crystal Structures

K. Nagata, N. Takeda,
N. Tokitoh* ◆

Gold–Xenon Complexes

T. Drews, S. Seidel, K. Seppelt*

Iron-Catalyzed Polyethylene Chain Growth on Zinc: Linear α -Olefins with a Poisson Distribution

G. J. P. Britovsek, S. A. Cohen,
V. C. Gibson,* P. J. Maddox,
M. van Meurs* ◆

Picture(s) of Fritz Haber: Rolf Hochhuth, Tony Harrison, and André Malraux—three very different writers—have portrayed Fritz Haber in their novels and plays. The picture may not please chemists. Several biographies and an essay by the historian Fritz Stern have also dealt with Haber's tragic life. Should we accept these as literary portraits, if they are not to our liking? Or struggle with them? And in Haber's case would this be justified?

Angew. Chem. **2001**, *113*, 4733–4739

R. Hoffmann, P. Laszlo . . . 4599–4604

Coping with Fritz Haber's Sombre Literary Shadow

Keywords: chemists in the literature • Haber, Fritz • history of chemistry • scientific ethics

What connects the author Marcel Proust, the Chemistry Nobel Laureate Henri Moissan, and the fraudulent engineer Henri François Lemoine? Moissan was obsessed with the idea of preparing artificial diamonds, Lemoine alleged that he had improved the Moissan technique, which only produced diamond dust, and Proust first invested a part of his wealth in the alleged diamond synthesis and then exploited the scandal in a literary work.

Angew. Chem. **2001**, *113*, 4739–4745

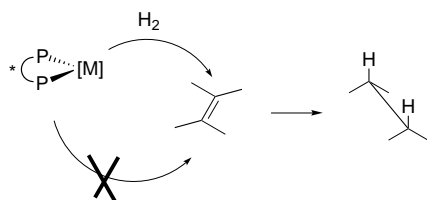
O. Krätz* . . . 4604–4610

The “Rocky” Road to Literary Fame: Marcel Proust and the Diamond Synthesis of Professor Moissan

Keywords: artificial diamonds • history of chemistry • Moissan, Henri

HIGHLIGHT

Far from being a well-understood reaction, the enantioselective hydrogenation of prochiral olefins with Rh- and Ru-bisphosphane catalysts (see picture, M = Rh, Ru) has recently shown some surprises. Among them are a catalytic cycle featuring initial addition of hydrogen to the catalyst and not the catalyst–substrate complex as well as a purely ionic mechanism.



Angew. Chem. **2001**, *113*, 4747–4749

K. Rossen* . . . 4611–4613

Ru- and Rh-Catalyzed Asymmetric Hydrogenations: Recent Surprises from an Old Reaction

Keywords: hydrogenation • P ligands • reaction mechanisms • rhodium • ruthenium

CORRESPONDENCE

Which scaling connects the number of conformers of a protein with the number of residues? The authors both explore this question and van Gunsteren et al. produce additional arguments to those in their original paper. Although the authors do not agree on the “scaling law”, they both acknowledge the importance of finding the correct answer as it has a great influence on the chance of simulating protein folding with reasonably good models.

Angew. Chem. **2001**, *113*, 4751–4752

Angew. Chem. **2001**, *113*, 4753–4754

A. R. Dinner, M. Karplus* 4615–4616

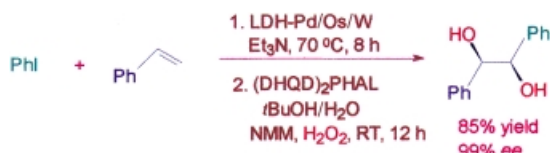
Comment on the Communication “The Key to Solving the Protein-Folding Problem Lies in an Accurate Description of the Denatured State” by van Gunsteren et al.

W. F. van Gunsteren,* R. Bürgi, C. Peter, X. Daura . . . 4617–4618

Reply

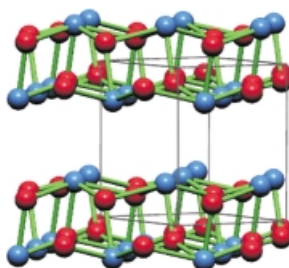
Keywords: computer chemistry • correspondence • molecular dynamics • peptides • protein folding

A transition metal based biomimic approach is used to realize multistep reactions, composed of multicomponent systems, in a single-pot synthesis of chiral diols mediated by a trifunctional (Pd, Os, W) catalyst anchored to a single matrix (see scheme; LDH = layered double hydroxide, (DHQD)₂PHAL = 1,4-bis(9-*O*-dihydroquinidiny)phthalazine, NMM = *N*-methylmorpholine).



Angew. Chem. **2001**, *113*, 4755–4759

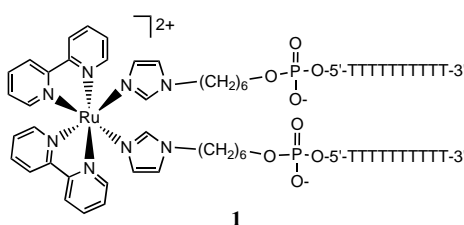
Even under a pressure of 46 GPa, the low-symmetry lone-pair structures of isoelectronic TlF and PbO (see picture for β -PbO), classic examples of systems with a stereochemically active lone pair, resist transformation into the corresponding high-symmetry NaCl and CsCl structures. Ab initio calculations allowed a simple bonding picture for lone-pair structures involving inert-pair elements to be developed.



Angew. Chem. **2001**, *113*, 4760–4765



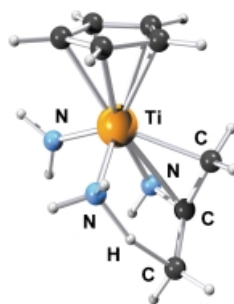
The branched DNA structure 1, in which a transition metal center resides at the branch point and joins two parallel DNA strands, was synthesized by a convergent solid-phase approach. Complex **1** efficiently hybridizes with complementary DNA to generate transition metal linked DNA duplexes. This opens the door to using the geometries of transition metal complexes to direct the association of DNA into novel motifs.



Angew. Chem. **2001**, *113*, 4765–4768

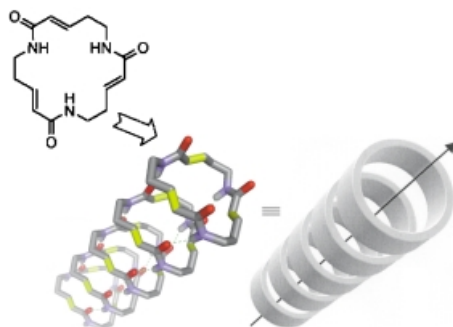


Proton transfer from ammine or amide ligands to vinylamine-type π systems in intermediary titanacycles (see picture) of allene and alkyne hydroamination reactions is predicted by DFT model calculations. The weaker coordination of alkenes to the Ti=N fragment, the lack of a π system in the titanacycle, and thus the necessity of direct Ti–C bond protonation rationalize a higher barrier for alkene hydroamination.



Angew. Chem. **2001**, *113*, 4768–4771

C₃-symmetric lactams in a tube: Specially designed rigid disc-shaped macrolactams self-assemble as endless tubes by means of backbone–backbone hydrogen bonds and van der Waals contacts (see scheme). All the tubes with very strong dipoles further aggregate in a parallel fashion and all the dipoles are still oriented in the same direction.



Angew. Chem. **2001**, *113*, 4771–4774

B. M. Choudary,* N. S. Chowdari,
S. Madhi, M. L. Kantam ... 4619–4623

A Trifunctional Catalyst for the Synthesis of Chiral Diols

Keywords: asymmetric synthesis • heterogeneous catalysis • immobilization • oxidation • transition metals

U. Häussermann,* P. Berastegui,
S. Carlson, J. Haines,
J.-M. Léger 4624–4629

TlF and PbO under High Pressure:
Unexpected Persistence of the
Stereochemically Active Electron Pair

Keywords: ab initio calculations • bond theory • high-pressure chemistry • layered compounds

I. Vargas-Baca, D. Mitra, H. J. Zolyniak,
J. Banerjee, H. F. Sleiman* 4629–4632

Solid-Phase Synthesis of Transition Metal
Linked, Branched Oligonucleotides

Keywords: DNA recognition • DNA structures • oligonucleotides • ruthenium

B. F. Straub,* R. G. Bergman* 4632–4635

The Mechanism of Hydroamination of
Allen, Alkynes, and Alkenes Catalyzed
by Cyclopentadienyltitanium–Imido
Complexes: A Density Functional Study

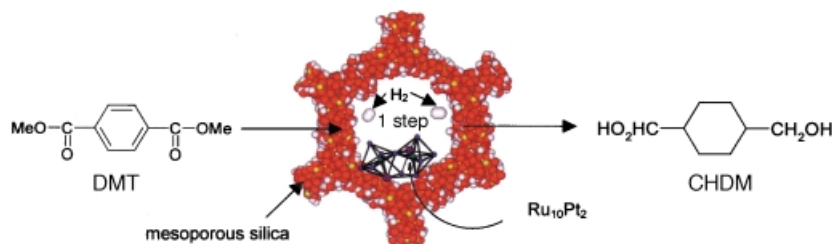
Keywords: density functional calculations • homogeneous catalysis • hydroamination • metallacycles • titanium

D. Gauthier, P. Baillargeon, M. Drouin,
Y. L. Dory* 4635–4638

Self-Assembly of Cyclic Peptides into
Nanotubes and Then into Highly
Anisotropic Crystalline Materials

Keywords: lactams • nanotubes • peptides • self-assembly • supramolecular chemistry

Pores for cluster catalysts: Nanoparticles of both Ru_5Pt and $\text{Ru}_{10}\text{Pt}_2$, uniformly distributed along the inner walls of mesoporous silica, exhibit high catalytic performance in the single-step hydrogenation of dimethyl terephthalate (DMT, to 1,4-cyclohexanedimethanol (CHDM); see scheme), of benzoic acid (to cyclohexane carboxylic acid), and of naphthalene (in the presence of sulfur) to *cis*-decalin.




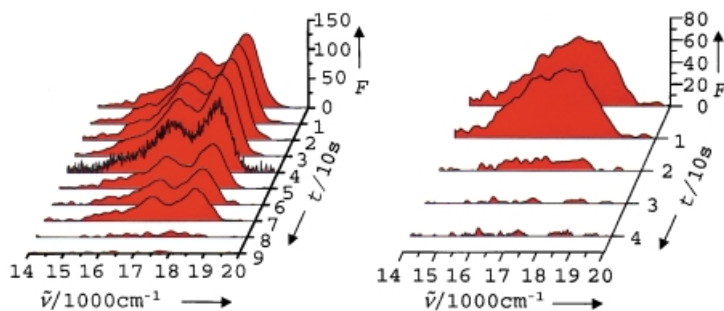
Angew. Chem. **2001**, *113*, 4774–4778

R. Raja, T. Khimyak, J. M. Thomas,*
S. Hermans,
B. F. G. Johnson* 4638–4642

Single-Step, Highly Active, and Highly Selective Nanoparticle Catalysts for the Hydrogenation of Key Organic Compounds

Keywords: cluster compounds • heterogeneous catalysis • hydrogenation • platinum • ruthenium

 **Collective on/off behavior** and different spectral behavior has been identified for individual molecules of different isomers (see for example the fluorescence spectra for two isomers as a function of time) with three perylenedicarboximide chromophores. In 8% of the dendrimer molecules, the chromophores interact to form an excimer-like structure which possess a higher rate of intersystem crossing than the rest of the molecules. This is the first time that this phenomenon has been proven experimentally at the single-molecule level.




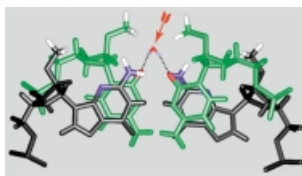
Angew. Chem. **2001**, *113*, 4779–4784

T. Vosch, J. Hofkens,* M. Cotlet, F. Köhn,
H. Fujiwara, R. Gronheid,
K. Van Der Biest, T. Weil, A. Herrmann,
K. Müllen, S. Mukamel,
M. Van der Auweraer,
F. C. De Schryver* 4643–4648

Influence of Structural and Rotational Isomerism on the Triplet Blinking of Individual Dendrimer Molecules

Keywords: chromophores • dendrimers • fluorescence spectroscopy • isomers • single-molecule spectroscopy

 **The simple replacement** of 2'-OH by 2'-OMe groups leads, in certain RNA structures, to a significant strengthening of important solute–solvent interactions. Molecular dynamics simulations uncover the complexity of effects associated with the insertion of hydrophobic groups into hydrophilic systems (the arrow indicates a long-lived bridging water molecule located in the shallow groove of a 2'-OMe(GpC) base pair step). Green = skeleton of cytosine, black = skeleton of guanine, red = oxygen atoms of water and of shallow groove carbonyl groups, blue = shallow groove nitrogen atoms, cyan = hydrogen atoms of OMe groups.



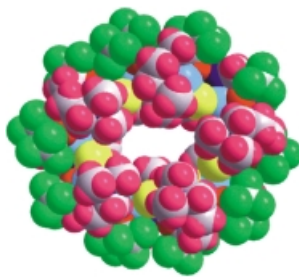
Angew. Chem. **2001**, *113*, 4784–4786

P. Auffinger,* E. Westhof* 4648–4650

Hydrophobic Groups Stabilize the Hydration Shell of 2'-O-Methylated RNA Duplexes

Keywords: computer chemistry • hydrophobic effect • molecular dynamics • nucleic acids • solvent effects

Copper gets into the ring: A decanuclear cyclic Cu^{II} complex is synthesized by direct treatment of CuCl_2 with a fluorinated amino alcoholate containing one secondary and one tertiary nitrogen donor (see space-filling diagram; Cu light blue, Cl yellow, O red, N dark blue, C gray). Possible factors that lead to the self-assembly of the unique molecular wheel are discussed.



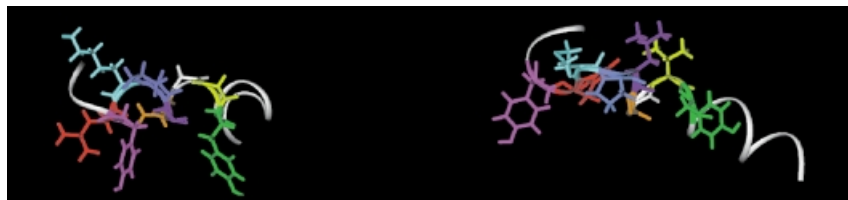
Angew. Chem. **2001**, *113*, 4787–4789

C.-H. Chang, K. C. Hwang, C.-S. Liu,
Y. Chi,* A. J. Carty,* L. Scoles,
S.-M. Peng,* G.-H. Lee,
J. Reedijk* 4651–4653

Formation and Stabilization of a
Decanuclear Cu^{II} Wheel Linked by
Chloride and $\text{O} \cdots \text{H}-\text{N}$ Hydrogen Bonds

Keywords: copper • hydrogen bonds •
magnetic properties • N,O ligands •
self-assembly

Rational design of a malaria vaccine may result from the structure–immunogenicity relationship of analogues of peptide 1585, a protein sequence located at the N-terminal end of the *P. falciparum* 42-kDa merozoite surface protein-1. Altering a few amino acids in peptide 1585 (left) induces immunogenicity and protectivity, and changes the 3D structure, as shown for one of the analogues synthesized (right).



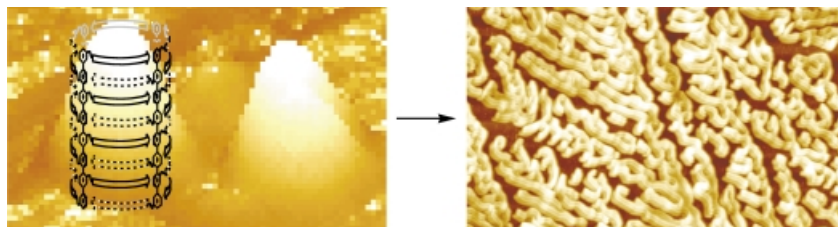
Angew. Chem. **2001**, *113*, 4790–4793

F. Espejo,* M. Cubillos, L. M. Salazar,
F. Guzman, M. Urquiza, M. Ocampo,
Y. Silva, R. Rodriguez, E. Lioy,
M. E. Patarroyo* 4654–4657

Structure, Immunogenicity, and
Protectivity Relationship for the 1585
Malarial Peptide and Its Substitution
Analogues

Keywords: immunochemistry • malaria •
NMR spectroscopy • protein
modification • protein structures

Delightful order and beauty is exhibited by novel supramolecular architectures constructed from preorganizing rigid-rod molecules which first self-assemble into β -barrel tertiary structures (left) and then transform into higher-order quaternary structures (right), that is, “rigid-rod β -fibrils”.



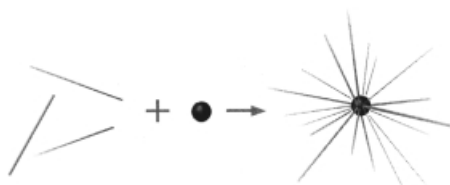
Angew. Chem. **2001**, *113*, 4793–4797

G. Das, L. Ouali, M. Adrian,
B. Baumeister, K. J. Wilkinson,
S. Matile* 4657–4661

β -Fibrillogenesis from Rigid-Rod
 β -Barrels: Hierarchical Preorganization
Beyond Microns

Keywords: atomic force microscopy •
nanostructures • oligomers • protein
models • supramolecular chemistry

A star is born: Size-selected, end-functionalized single-walled carbon nanotubes react with amine-terminated dendrimers to form star-shaped objects (see schematic representation). Analysis of the nanotube stars by atomic force microscopy and scanning electron microscopy show that they exhibit a peculiar response to electron beams.



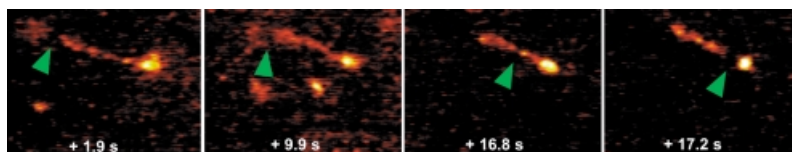
Angew. Chem. **2001**, *113*, 4797–4799

M. Sano,* A. Kamino,
S. Shinkai 4661–4663

Construction of Carbon Nanotube “Stars”
with Dendrimers

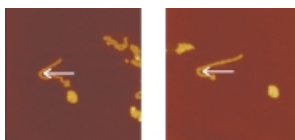
Keywords: dendrimers • nanostructures •
nanotubes • scanning probe microscopy

A slice of life: Individual, fluorescently labeled DNA molecules are cut by a restriction enzyme into a sequence-specific fingerprint-like pattern and the time course of the reaction is analyzed by fluorescence microscopy. As shown in the picture, all the cuts occur one after another from one end to the other along the DNA molecule.



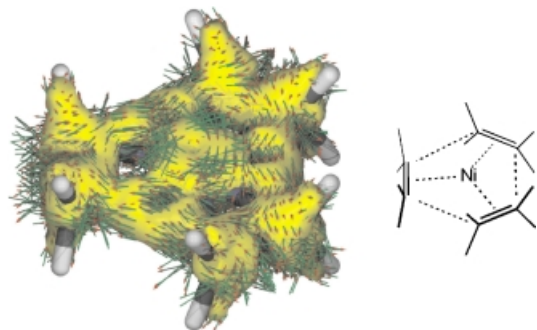
Angew. Chem. **2001**, *113*, 4799–4802

Moving individual molecules: Up to 250-nm long polystyrene chains with fourth generation dendrons at each repeat unit were synthesized, individualized on highly oriented pyrolytic graphite (HOPG), and manipulated into a stretched linear conformation by a scanning force microscope tip (see images, arrow indicates direction of movement).



Angew. Chem. **2001**, *113*, 4802–4805

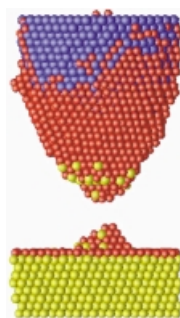
An ACID test for aromaticity: A number of criteria prove that tris(ethylene)nickel(0) and tris(ethyne)nickel(0) are aromatic compounds. The ligands strongly interact in the periphery and are “on the way” to trimerizing to cyclohexane and benzene, respectively. The electronic structure of these complexes (see picture, which shows the current density vectors plotted onto the ACID surface of the nickel ethylene complex) sheds light upon the role of Ni^0 as a catalyst in cyclooligomerization reactions. ACID = anisotropy of the induced current density; a method for visualizing the density of delocalized electrons and for quantifying conjugation effects.



Angew. Chem. **2001**, *113*, 4809–4813



The fabrication of small metal clusters with a scanning tunneling microscope in an electrochemical environment has been simulated with a computer. (The picture shows the copper-covered tip of the scanning tunneling microscope above the Au(111) surface, which is covered by copper.) In the case of copper deposition on Au(111), Cu–Au clusters were formed that are more stable than pure copper. The simulations suggest that the formation of stable clusters by this method can only succeed if the deposited metal and the substrate form a stable alloy.



Angew. Chem. **2001**, *113*, 4807–4809

B. Schäfer, H. Gemeinhardt,
K. O. Greulich* 4663–4666

Direct Microscopic Observation of the
Time Course of Single-Molecule DNA
Restriction Reactions

Keywords: DNA restriction • enzyme
catalysis • fluorescence microscopy •
optical tweezers • single molecules

L. Shu, A. D. Schlüter,* C. Ecker,
N. Severin, J. P. Rabe* 4666–4669

Extremely Long Dendronized Polymers:
Synthesis, Quantification of Structure
Perfection, Individualization, and SFM
Manipulation

Keywords: amines • dendrimers •
polymerization • scanning force
microscopy

R. Herges,*
A. Papafilippopoulos 4671–4674

Homoaromaticity in
Tris(ethylene)nickel(0) and
Tris(ethyne)nickel(0)

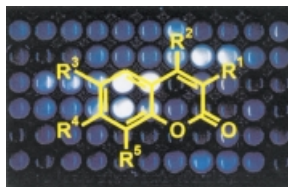
Keywords: aromaticity • electronic
structure • magnetic properties •
nickel • through-space interactions

M. G. Del Pópolo, E. P. M. Leiva,*
W. Schmickler* 4674–4676

On the Stability of Electrochemically
Generated Nanoclusters—A Computer
Simulation

Keywords: alloys • cluster compounds •
electrochemistry • molecular dynamics •
scanning tunneling microscopy

“Hits” with high quantum yields: The screening of the chromophores of a coumarin library for optical properties allowed the identification of “hits” with high fluorescence quantum yields (see picture) which could be used as fluorescence labels and laser dyes. The generation of the library was facilitated by an efficient method involving the parallel synthesis utilizing Pd-catalyzed cross-coupling reactions.



M.-S. Schiedel, C. A. Briehn,
P. Bäuerle* 4677–4680

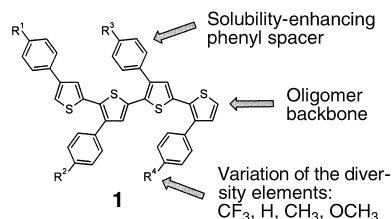
Single-Compound Libraries of Organic
Materials: Parallel Synthesis and
Screening of Fluorescent Dyes

Keywords: coumarins • combinatorial
chemistry • cross-coupling •
fluorescence • high-throughput screening

Angew. Chem. **2001**, *113*, 4813–4816



256 oligomers make up the quater-thiophene library of compounds **1** which was prepared by a combination of parallel and “mix-and-split” syntheses. An automated screening process for the recording of cyclic voltammetric data and subsequent data analysis allowed the development of structure–property relationships on which to base the future design of π -conjugated oligomers.



C. A. Briehn, M.-S. Schiedel,
E. M. Bensen, W. Schuhmann,
P. Bäuerle* 4680–4683

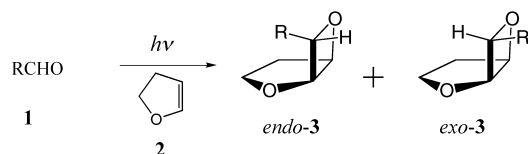
Single-Compound Libraries of Organic
Materials: From the Combinatorial
Synthesis of Conjugated Oligomers to
Structure–Property Relationships

Keywords: combinatorial chemistry •
conducting materials • cross-coupling •
cyclic voltammetry • high-throughput
screening

Angew. Chem. **2001**, *113*, 4817–4820



The multiplicity of the excited state controls the product distribution in the formation of *endo/exo*-oxetane **3** in the photocycloaddition of aldehydes **1** ($R = \text{Ph, Et, Me, } i\text{Bu}$) with dihydrofuran **2** (Paternò–Büchi reaction). Whether the singlet or triplet channel dominates is strongly dependent on the temperature, which is therefore critical for the selectivity of the reaction.



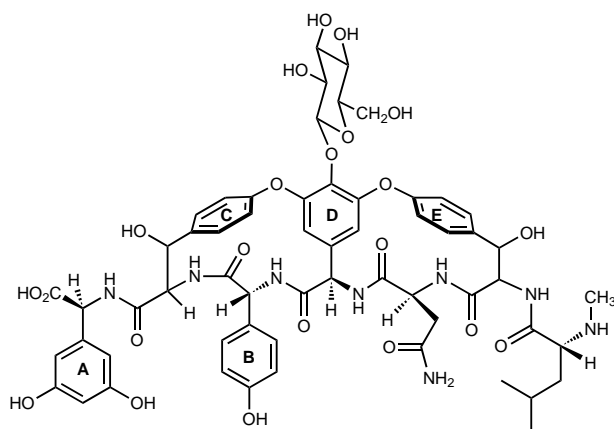
A. G. Griesbeck,* S. Bondock,
M. S. Gudipati* 4684–4687

Temperature and Viscosity Dependence
of the Spin-Directed Stereoselectivity of
the Carbonyl–Alkene Photocycloaddition

Keywords: diastereoselectivity •
isoinversion principle • photochemistry •
photocycloaddition • radical reaction

Angew. Chem. **2001**, *113*, 4828–4832

Linear and bicyclic glycopeptides occur as intermediates in the biosynthesis of the aglycon of glycopeptide antibiotics of the type shown. Considering the structures of these peptides and those of previously isolated analogues, the sequence of the three oxidative ring-closing steps can be deduced for type-I and type-II glycopeptide antibiotics. Thus, comprehensive insight into the assembly of the aglycon is achieved for the first time.



D. Bischoff, S. Pelzer, B. Bister,
G. J. Nicholson, S. Stockert, M. Schirle,
W. Wohlleben, G. Jung,
R. D. Süssmuth* 4688–4691

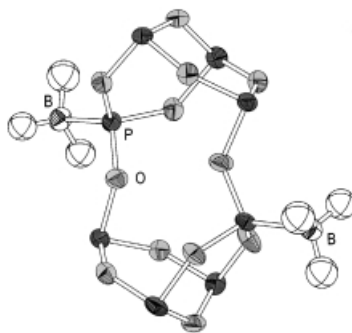
The Biosynthesis of Vancomycin-Type
Glycopeptide Antibiotics—The Order of
the Cyclization Steps

Keywords: antibiotics • balhimycin •
biosynthesis • glycopeptides •
vancomycin

Angew. Chem. **2001**, *113*, 4824–4827

Ambivalent chemical reactivity is characteristic for molecular phosphorus oxides: They either react in a vigorous and uncontrolled manner or they are practically inert, for example, in attempts at controlled ring-opening reactions. Thus, the spontaneous dimerization of $\text{P}_4\text{O}_6 \cdot \text{BH}_3$ to give $\text{P}_8\text{O}_{12} \cdot 2\text{BH}_3$ (see crystal structure) is a real surprise.


Angew. Chem. **2001**, *113*, 4838–4840

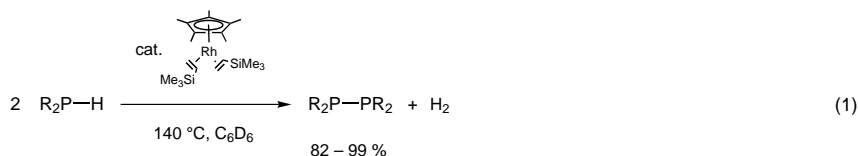


A. Tellenbach, M. Jansen* 4691–4694

Dimerization of Molecular Phosphorus Oxides

Keywords: cage compounds • mass spectrometry • phosphorus • phosphorus oxides • solid-state structures

 **Two reaction protocols** have been developed for the catalytic dehydrocoupling of secondary phosphanes by the rhodium(i) complex $[\text{Cp}^*\text{Rh}\{\text{CH}_2=\text{CH}(\text{TMS})\}_2]$: In the presence of an olefin, transfer hydrogenation occurs to give the corresponding alkane and the diphosphane. Without the addition of an olefin, the reaction proceeds by loss of dihydrogen but more elevated reaction temperatures must be used [Eq. (1)].



Angew. Chem. **2001**, *113*, 4832–4834

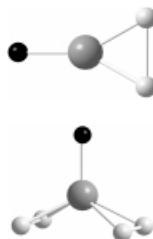
V. P. W. Böhm,
M. Brookhart* 4694–4696

Dehydrocoupling of Phosphanes
Catalyzed by a Rhodium(i) Complex

Keywords: homogeneous catalysis • phosphanes • P–H activation • P–P coupling • rhodium

A photolytically induced reaction of AlF with O_2 in an argon matrix afforded the first peroxo and bis-superoxo complexes of aluminum: FAIO_2 and $\text{FAI}(\text{O}_2)_2$ (see picture). The compounds were identified and characterized by IR spectroscopy and density functional theory (DFT) as well as ab initio calculations.

Angew. Chem. **2001**, *113*, 4820–4824

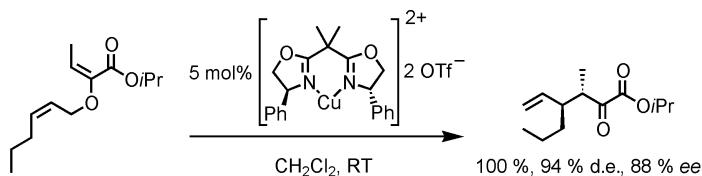


J. Bahlo, H.-J. Himmel,
H. Schnöckel* 4696–4700

The First Detection of Peroxo and Bis-superoxo Complexes of Aluminum:
 FAIO_2 and FAIO_4

Keywords: aluminum • matrix isolation • peroxo ligands • photolysis • superoxo ligands

Almost 90 years after it was first described by Ludwig Claisen, a catalyzed enantioselective Claisen rearrangement has been implemented for the first time. Chiral copper(II) bis(oxazolines) catalyzed the Claisen rearrangement of 2-alkoxycarbonyl-substituted allyl vinyl ethers with enantiomeric excesses of 80–90% (see scheme).



Angew. Chem. **2001**, *113*, 4835–4837

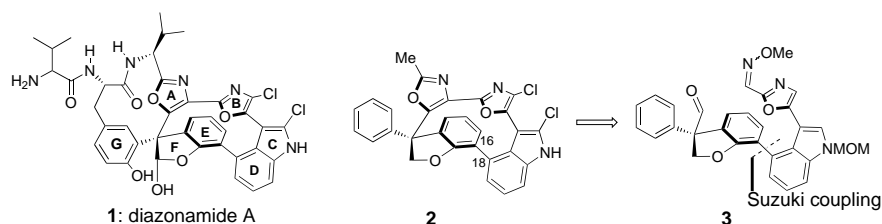
L. Abraham, R. Czerwonka,
M. Hiersemann* 4700–4703

The Catalytic Enantioselective Claisen
Rearrangement of an Allyl Vinyl Ether

Keywords: asymmetric catalysis • enantioselectivity • ketones • copper • rearrangements



One of the most enticing natural products isolated in recent years and a serious challenge to synthetic chemists is represented by the potent anticancer agent diazonamide A (**1**). By utilizing a highly convergent approach, the ABCDEF macrocycle **2** was constructed in only 16 linear steps based on a key intermolecular Suzuki coupling reaction to generate the C₁₆–C₁₈ biaryl linkage and a remarkable SmI₂-induced hetero pinacol coupling cascade sequence.



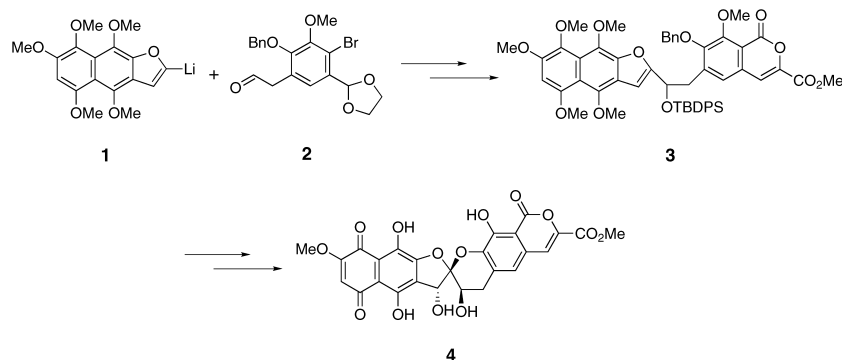
Angew. Chem. **2001**, *113*, 4841–4845

K. C. Nicolaou,* X. Huang,
N. Giuseppone, P. Bheema Rao, M. Bella,
M. V. Reddy, S. A. Snyder 4705–4709

Construction of the Complete Aromatic
Core of Diazonamide A by a Novel
Hetero Pinacol Macrocyclization
Cascade Reaction

Keywords: C–C coupling • cyclization •
heterocycles • natural products •
samarium diiodide

A strategy for the synthesis of heliquinomycin, a selective helicase inhibitor, hinges on the spirocyclization of precursor **3**. Naphthofuran **1** and aldehyde **2** were readily prepared and used in the synthesis of **3**. The key steps in the total synthesis of heliquinomycinone (**4**) include the regioselective dihydroxylation of **3**, and a novel spirocyclization under Mitsunobu conditions.



Angew. Chem. **2001**, *113*, 4845–4849

Angew. Chem. **2001**, *113*, 4849–4852

D. Qin, R. X. Ren, T. Siu, C. Zheng,
S. J. Danishefsky* 4709–4713

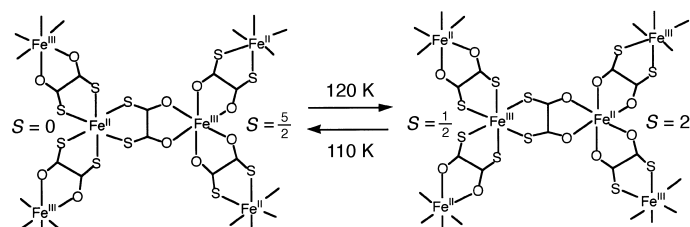
Studies in the Total Synthesis of
Heliquinomycinone: Proof of Concept
and Assembly of a Fully Mature
Spirocyclization Precursor

T. Siu, D. Qin,
S. J. Danishefsky* 4713–4716

The Total Synthesis of
Heliquinomycinone

Keywords: antitumor agents •
dihydroxylation • quinones •
spiro compounds • total synthesis

Not a classical spin-crossover: The heat capacity of the mixed-valence complex $\{[(n\text{-C}_3\text{H}_7)_4\text{N}][\text{Fe}^{\text{II}}\text{Fe}^{\text{III}}(\text{dto})_3]\}_\infty$ (dto = dithiooxalato, see scheme) exhibits a phase transition at 122.4 K as a result of electron transfer, and gives insight into the cooperative phenomena exhibited by the multifunctional material.



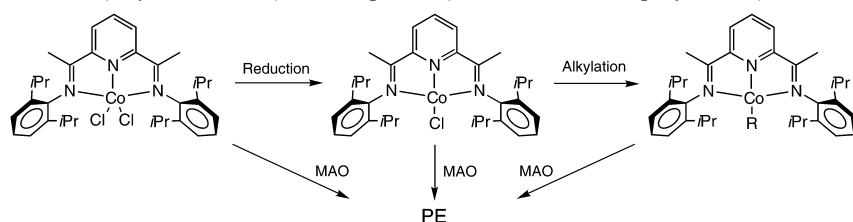
Angew. Chem. **2001**, *113*, 4852–4855

T. Nakamoto, Y. Miyazaki, M. Itoi,
Y. Ono, N. Kojima,*
M. Sorai* 4716–4719

Heat Capacity of the Mixed-Valence
Complex $\{[(n\text{-C}_3\text{H}_7)_4\text{N}][\text{Fe}^{\text{II}}\text{Fe}^{\text{III}}(\text{dto})_3]\}_\infty$,
Phase Transition because of Electron
Transfer, and a Change in Spin-State of
the Whole System

Keywords: electron transfer • iron •
mixed-valence compounds • O,S ligands •
phase transitions

Activated by reduction: On treatment with methylaluminoxane (MAO), the Brookhart/Gibson cobalt-based polymerization precatalyst $[\text{LCo}^{\text{II}}\text{Cl}_2]$ is first reduced to $[\text{LCo}^{\text{I}}\text{Cl}]$, subsequently alkylated to $[\text{LCo}^{\text{I}}\text{Me}]$, and finally converted into the (as yet unknown) active species (see scheme, PE = polyethylene).



Angew. Chem. **2001**, *113*, 4855–4858

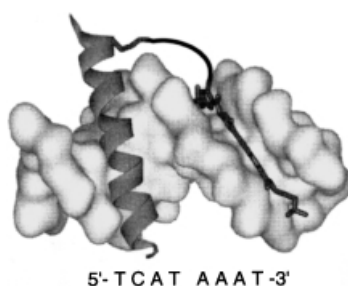
T. M. Kooistra, Q. Knijnenburg,
J. M. M. Smits, A. D. Horton,
P. H. M. Budzelaar,
A. W. Gal* 4719–4722

Olefin Polymerization with
[[bis(imino)pyridyl] $\text{Co}^{\text{II}}\text{Cl}_2$]: Generation
of the Active Species Involves Co^{I}

Keywords: alkylation • cobalt •
homogeneous catalysis • N ligands •
polymerization



A bivalent system capable of binding to hybrid DNA sites through simultaneous interaction in the major and the minor groove (see schematic representation) is formed by appropriate linking of the basic region of a b-ZIP protein (GCN4) to a tripyrrole related to the antibiotic distamycin.



Angew. Chem. **2001**, *113*, 4859–4861

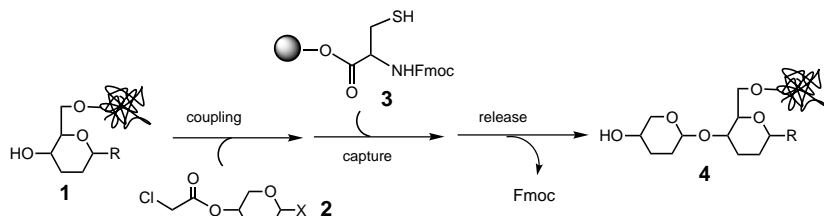
M. E. Vázquez, A. M. Caamaño,
J. Martínez-Costas, L. Castedo,
J. L. Mascareñas* 4723–4725

Design and Synthesis of a Peptide That
Binds Specific DNA Sequences through
Simultaneous Interaction in the Major
and in the Minor Groove

Keywords: antibiotics • DNA
recognition • peptides



A highly simplified synthesis of a tetrasaccharide was possible by a repeated coupling/capture–release cycle. In the first cycle, a glycosyl acceptor (**1**) bound to a soluble polymer reacted with a glycosyl donor (**2**) having a chloroacetyl group as a temporary protecting group. Solid-phase capture by a resin-bound thiol group (in **3**) was followed by Fmoc removal, which released the polymer-bound disaccharide **4** into the solution phase. Fmoc = 9-fluorenylmethoxycarbonyl.



Angew. Chem. **2001**, *113*, 4861–4864

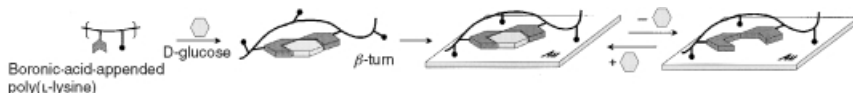
H. Ando, S. Manabe, Y. Nakahara,
Y. Ito* 4725–4728

Solid-Phase Capture–Release Strategy
Applied to Oligosaccharide Synthesis on
a Soluble Polymer Support

Keywords: glycosylation •
oligosaccharides • polymer support •
solid-phase synthesis



The dominant solution-phase conformation of a polymer can be fixed to a surface (see scheme). Boronic acid appended poly(L-lysine) assumes different conformations in the presence of D-glucose or D-fructose. When the polymer–glucose complex is anchored to a gold surface, an imprinted interface with “molecular memory” for glucose over fructose can be prepared.



Angew. Chem. **2001**, *113*, 4865–4867

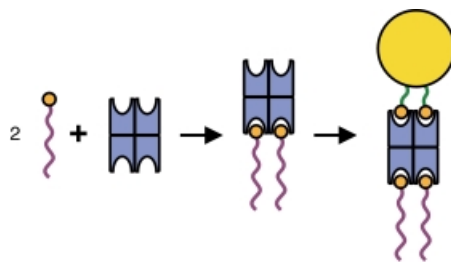
A. Friggeri, H. Kobayashi, S. Shinkai,*
D. N. Reinhoudt* 4729–4731

From Solutions to Surfaces: A Novel
Molecular Imprinting Method Based on
the Conformational Changes of Boronic-
Acid-Appended Poly(L-lysine)

Keywords: molecular recognition •
carbohydrates • surface chemistry



Association of streptavidin and two biotinylated polystyrene chains to form protein–polymer hybrids results in “giant amphiphiles” (see first step of schematic representation). Functionality can be introduced by the complexation of other biotinylated molecules to the remaining binding sites of streptavidin (second step).



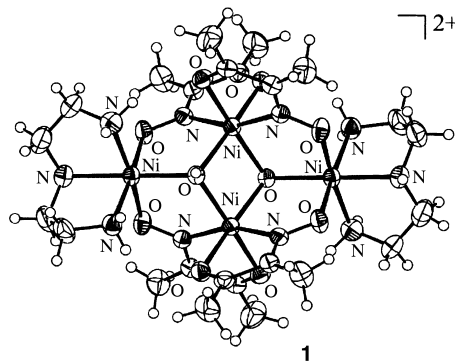
J. M. Hannink, J. J. L. M. Cornelissen,
J. A. Farrera, P. Foubert,
F. C. De Schryver,
N. A. J. M. Sommerdijk,
R. J. M. Nolte * 4732–4734

Protein–Polymer Hybrid Amphiphiles

Keywords: aggregation • amphiphiles •
monolayers • polymers • proteins

Angew. Chem. **2001**, *113*, 4868–4870

A Ni_4O_2 core based on a “chair” topology forms the central unit of the tetranuclear nickel(II) complex **1**, which possesses $\mu_3\text{-OH}^-$ and butane-2,3-dione-monooximate bridges and displays fascinating magnetic properties. The major Ni–Ni interactions in **1** are antiferromagnetic in nature, and the large $\text{Ni}_{\text{core}}\text{-O-Ni}_{\text{terminal}}$ angle in the core is responsible for driving all the Ni_{core} spins parallel.



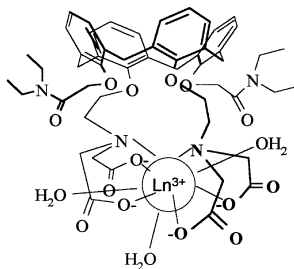
V. V. Pavlishchuk,* S. V. Kolotilov,
A. W. Addison,* M. J. Prushan,
D. Schollmeyer, L. K. Thompson,
E. A. Goreshnik 4734–4737

A Tetrameric Nickel(II) “Chair” with both
Antiferromagnetic Internal Coupling and
Ferromagnetic Spin Alignment

Keywords: magnetic properties • nickel •
oximes

Angew. Chem. **2001**, *113*, 4870–4873

Contrasting calixarenes: Thermodynamically stable and water-soluble calix[4]arene– Ln^{III} (see picture) complexes may represent a new class of relaxation ($\text{Ln} = \text{Gd}$) or luminescent ($\text{Ln} = \text{Eu}$, Tb) probes for biomedical studies. The first complete characterization of one of these complexes in water is reported. The Gd^{III} chelate shows a strong binding affinity with human serum albumin as a result of the cooperative effects of hydrophobic interaction and coordination by donors groups on the protein.



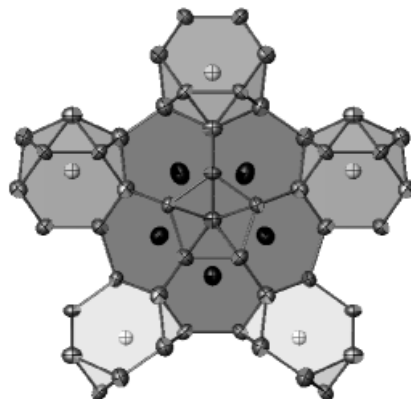
S. Aime, A. Barge, M. Botta,*
A. Casnati,* M. Fragai, C. Luchinat,
R. Ungaro 4737–4739

A Calix[4]arene Gd^{III} Complex Endowed
with High Stability, Relaxivity, and
Binding Affinity to Serum Albumin

Keywords: calixarenes • contrast agents •
coordination chemistry • lanthanides •
NMR spectroscopy

Angew. Chem. **2001**, *113*, 4873–4875

A pseudo-pentagonal kernel is the central unit in the new quaternary intermetallic phase $\text{Li}_{10}\text{Mg}_6\text{Zn}_{31}\text{Al}_3$ (see structure). This unit can form the basis for decagonal and, possibly, icosahedral quasicrystals. The synthesis, crystal structure, and bonding of $\text{Li}_{10}\text{Mg}_6\text{Zn}_{31}\text{Al}_3$ are discussed in detail.



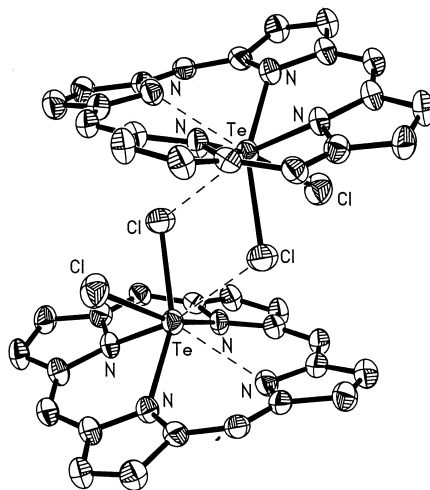
C.-S. Lee, G. J. Miller* 4740–4742

$\text{Li}_{10}\text{Mg}_6\text{Zn}_{31}\text{Al}_3$: A New Intermetallic
Phase Containing Building Blocks for
Decagonal Quasicrystals

Keywords: electronic structure •
intermetallic phases • quasicrystals •
solid-state structures

Angew. Chem. **2001**, *113*, 4876–4878

An unusual bonding mode for a porphyrin ligand is seen in the tellurium porphyrin complex prepared by treatment of TeCl_4 with dilithio *meso*-tetra(*p*-tolyl)porphyrin [$\text{Li}_2(\text{ttp})$]. The structure of $[\text{Te}(\text{ttp})\text{Cl}_2]$ (see picture) has a five-coordinate, square-pyramidal geometry involving a distorted tridentate porphyrin ligand and *cis*-dichloride ligands.



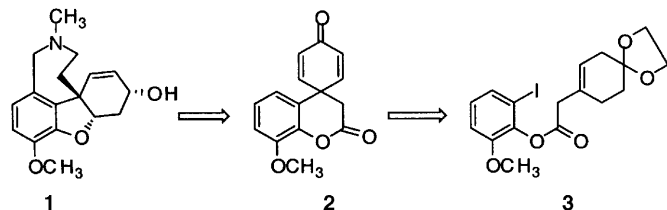
Angew. Chem. **2001**, *113*, 4879–4881

D. S. Grubisha, I. A. Guzei, N. Al-Salim,
P. D. W. Boyd, P. J. Brothers,*
L. K. Woo* 4743–4745

Novel Coordination in the First Tellurium Porphyrin Complex: Synthesis and Crystal Structure of $[\text{Te}(\text{ttp})\text{Cl}_2]$

Keywords: coordination chemistry • macrocyclic ligands • porphyrinoids • structure elucidation • tellurium

Intramolecular Heck reaction of **3** generates a spiro quaternary C atom—a key step in an efficient synthesis of galanthamine (**1**). Galanthamine can be readily obtained from the spiro tricyclic dienone **2**, which was prepared by nonclassical dehydrogenation of the corresponding α,β -unsaturated ketone.



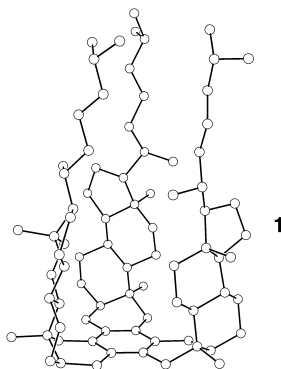
Angew. Chem. **2001**, *113*, 4881–4882

C. Guillou,* J.-L. Beunard, E. Gras,
C. Thal* 4745–4746

An Efficient Total Synthesis of (\pm)-Galanthamine

Keywords: alkaloids • Heck reaction • natural products • spiro compounds • total synthesis

Starting from coprostanone with a *cis* A/B ring fusion, the basis for a new class of enantioselective hosts has been established. The trimerization by $\text{TiCl}_4/\text{ZnCl}_2$ gave the tri-steroid **1**, a C_3 -symmetric hydrocarbon that, according to X-ray analysis, contains a deep, chiral cleft.



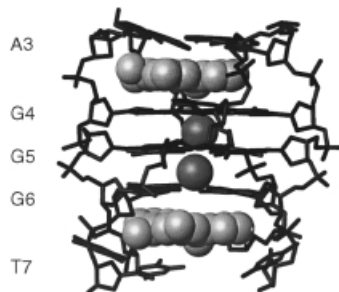
Angew. Chem. **2001**, *113*, 4882–4884

R. A. Pascal, Jr.,* M. S. Mathai, X. Shen,
D. M. Ho 4746–4748

Trimerization of a Steroid Ketone To Form a Chiral Molecular Cleft

Keywords: chirality • cyclotrimerization • polycycles • steroids

Guided by 24 drug–DNA NOEs, the complex formed between RHPS4 (a novel fluorinated polycyclic methylacridinium salt with potent telomerase activity) and $d(\text{TTAGGGT})_4$ has been modeled by using MD simulations with drug molecules intercalated at the ApG and GpT steps. A low-energy structure for the 2:1 complex has a partial positive charge on the acridine 13-N atom (which acts as a pseudo potassium ion) positioned above the center of the G-tetrad (see picture).



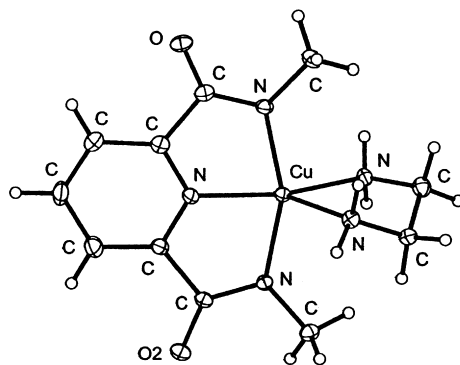
Angew. Chem. **2001**, *113*, 4885–4887

E. Gavathiotis, R. A. Heald,
M. F. G. Stevens,
M. S. Searle* 4749–4751

Recognition and Stabilization of Quadruplex DNA by a Potent New Telomerase Inhibitor: NMR Studies of the 2:1 Complex of a Pentacyclic Methylacridinium Cation with $d(\text{TTAGGGT})_4$

Keywords: DNA recognition • G-quadruplex • NMR spectroscopy • telomerase

Acetonitrile might not be an “innocent” solvent after all: The monomeric Cu^{II} complex $[\text{Cu}(\text{dmppy})(\text{en})]$ (see structure) readily cleaves the C–C bond of acetonitrile under ambient conditions. Previously, heterolytic cleavage of the C–C bond of acetonitrile had only been achieved by phosphane complexes of metals in low oxidation states. $\text{dmppyH}_2 = N,N'$ -dimethylpyridine-2,6-dicarboxamide, $\text{en} = \text{ethylenediamine}$.



D. S. Marlin, M. M. Olmstead,
P. K. Mascharak* 4752–4754

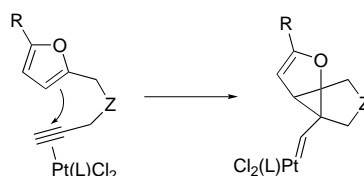
Heterolytic Cleavage of the C–C Bond of Acetonitrile with Simple Monomeric Cu^{II} Complexes: Melding Old Copper Chemistry with New Reactivity

Keywords: acetonitrile • cleavage reaction • copper • cyanides • N ligands

Angew. Chem. **2001**, *113*, 4888–4890



A platinum cyclopropyl carbene complex, formed by *anti* attack of the furan ring on an $(\eta^2\text{-alkyne})\text{Pt}^{\text{II}}$ complex (see scheme), is the key intermediate in the intramolecular reaction of furans with alkynes according to experimental studies and density functional calculations.



B. Martín-Matute, D. J. Cárdenas,
A. M. Echavarren* 4754–4757

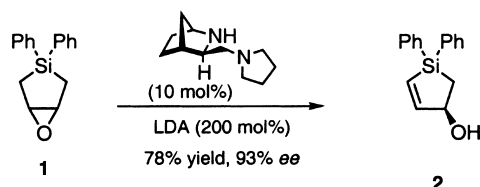
Pt^{II} -Catalyzed Intramolecular Reaction of Furans with Alkynes

Keywords: alkynes • cycloaddition • density functional calculations • heterocycles • platinum

Angew. Chem. **2001**, *113*, 4890–4893



A versatile precursor for the assembly of a range of polyol-containing fragments is the silacyclic alcohol **2** that results from the highly enantioselective, catalytic isomerization of diphenylsilacyclopentene oxide (**1**). The use of this precursor is illustrated with the efficient and highly diastereoselective assembly of acyclic tetraol motifs.



D. Liu, S. A. Kozmin* 4757–4759

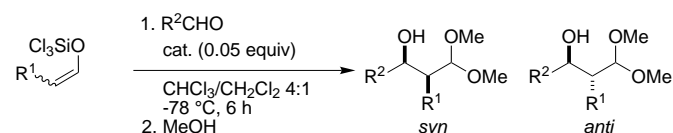
Catalytic Enantioselective Isomerization of Silacyclopentene Oxides: New Strategy for Stereocontrolled Assembly of Acyclic Polyols

Keywords: amides • base catalysis • epoxides • polyols • silanes

Angew. Chem. **2001**, *113*, 4893–4895



The most basic of aldol constructions, namely the controlled stereoselective self-condensation of aldehydes, has finally found a general solution. Geometrically defined trichlorosilyl enolates of aldehydes display excellent reactivity, near perfect diastereoselectivity, and good (albeit variable) enantioselectivity in their addition to a wide range of aldehydes under catalysis by a chiral bisphosphoramidate (see scheme).



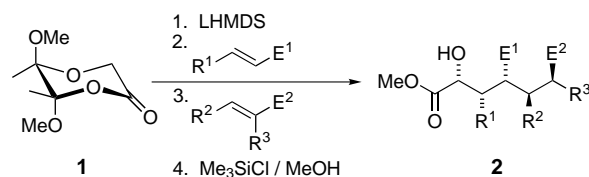
S. E. Denmark,*
S. K. Ghosh 4759–4762

The First Catalytic, Diastereoselective, and Enantioselective Crossed-Aldol Reactions of Aldehydes

Keywords: aldol reaction • diastereoselectivity • enantioselectivity • Lewis base catalysis

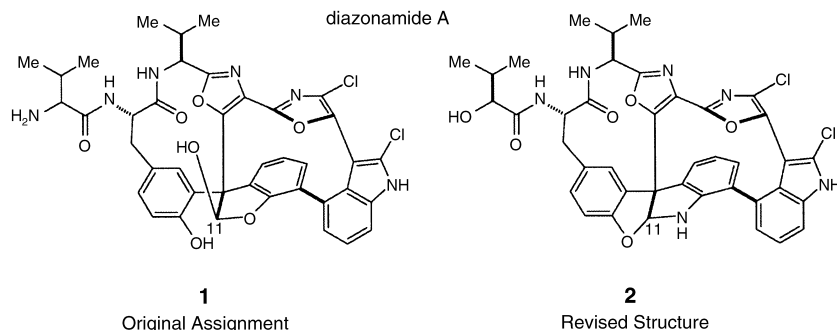
Angew. Chem. **2001**, *113*, 4895–4898

Up to five new stereogenic centers (see **2**) can be formed in one-pot consecutive three- and four-component coupling reactions starting from a butane diacetal desymmetrized glycolic acid derivative **1**. Highly functionalized α -hydroxy acid derivatives are obtained in an easy, fast, clean, and efficient way. LHMDS = lithium hexamethyldisilazide.



Angew. Chem. **2001**, *113*, 4899–4901

Unable to bear the weight of scrutiny, the original structure proposed for (–)-diazonamide A (**1**) must be revised. A convergent, stereocontrolled total synthesis provided **1**, which shows altered physical and spectroscopic characteristics relative to those of a sample of the natural product. Reinterpretation of reported data and new insight indicate that the actual structure of diazonamide A is the aminal-containing (*S*)- α -hydroxy isovaleric acid conjugate **2**. Gratifyingly, a synthetic C11 acetal congener of **2** is, by all biological measures examined, similarly potent and functionally equivalent to the antimitotic natural product.



Angew. Chem. **2001**, *113*, 4901–4904

Angew. Chem. **2001**, *113*, 4905–4909

Supporting information on the WWW
(see article for access details).

D. J. Dixon, S. V. Ley,*
F. Rodríguez 4763–4765

Consecutive Three- and Four-Component
Coupling Reactions with Anions
Generated from a Butane Diacetal
Desymmetrized Glycolic Acid Derivative

Keywords: acetals • asymmetric
synthesis • C–C coupling • Michael
addition • synthetic methods

J. Li, S. Jeong, L. Esser,
P. G. Harran* 4765–4769

Total Synthesis of Nominal
Diazonamides—Part 1: Convergent
Preparation of the Structure Proposed for
(–)-Diazonamide A

J. Li, A. W. G. Burgett, L. Esser,
C. Amezcua, P. G. Harran* 4770–4773

Total Synthesis of Nominal
Diazonamides—Part 2: On the True
Structure and Origin of Natural Isolates

Keywords: antitumor agents •
natural products • photochemistry •
rearrangements • total synthesis

* Author to whom correspondence should be addressed

SERVICE

- | | | | |
|---------------------------------------|------------------|------------------|-------------|
| • VIPs | 4522 | • Authors | 4775 |
| • Angewandte's Sister-Journals | 4539–4541 | • Preview | 4776 |
| • Vacancies | A143 | • Indexes | 4779 |
| • Keywords | 4774 | | |

Issue 23, 2001 was published online on November 28

**Don't forget all the Tables of Contents
from 1998 onwards may be still found
on the WWW under:
<http://www.angewandte.com>**